Construction of a top-loading adiabatic calorimeter and enthalpy relaxation of glassy (1,3-propanediol)$_{0.5}$(1,2-propanediamine)$_{0.5}$

Itaru Tsukushi,[a] Osamu Yamamuro,[b] Keishi Sadanami,[c] Makoto Nishizawa, and Takasuke Matsuo
Department of Chemistry and Microcalorimetry Research Center, Graduate School of Science, Osaka University, 1-1 Machikaneyama-cho, Toyonaka, Osaka 560, Japan

Kiyoshi Takeda
Department of Chemistry, Naruto University of Education, Naruto, Tokushima 772, Japan

(Received 18 August 1997; accepted for publication 20 October 1997)

We have developed a top-loading type adiabatic calorimeter which works in the temperature range 13–375 K. This calorimeter drastically reduces the time required for the sample setup (to ~10 min) and enables us to set up samples at liquid nitrogen temperature (77 K). The heat capacity of an empty cell was measured in a test experiment. The imprecision of the heat capacity measurement was ±0.2% at 13–30 K, ±0.1% at 30–50 K, and ±0.02% at above 50 K. These are as good as the performance of any of the traditional adiabatic calorimeters. The heat capacity of (1,3-propanediol)$_{0.5}$(1,2-propanediamine)$_{0.5}$ was measured in the temperature range 20–290 K and the enthalpy relaxation in its glassy state was also measured near $T_g(=178\ \mathrm{K})$. Because of the top-loading feature, fast-quenched samples prepared at 77 K outside the cryostat could be set up without ever undergoing a temperature above 100 K. © *1998 American Institute of Physics.* [S0034-6748(98)04301-9]

I. INTRODUCTION

The adiabatic calorimetry is one of the most powerful and versatile methods for studying physical properties of condensed matter. It provides absolute values of the heat capacity as a function of temperature with an imprecision of less than 0.1%. The Gibbs energy derived from the heat capacity is a quantity of prime importance in chemical thermodynamics, determining the relative stability of the phases of a substance. To this classical role of the adiabatic calorimetry has been added a new type of thermal measurement to determine slow evolution of heat that takes place in 10^2-10^6 s in a sample kept under an adiabatic condition. This enables one to study thermodynamic aspects of various irreversible changes such as glass transitions, crystallization, and phase separation.

The top-loading type cryostat is widely used in various low-temperature experiments, such as spectroscopic, electrical, or magnetic measurements. The merit of such a cryostat is that samples can be set up in the apparatus with a simple operation and then cooled quickly down to the desired low temperature, enhancing the efficiency of the low-temperature experiments. This merit is quite substantial for the experiments at expensive public facilities, such as neutron scattering.

In the present context, the quick loading feature enables us to do a new type of experiment in which the samples prepared in advance at low temperatures are set up at low temperature. There are many interesting substances which can be studied only by the top-loading cryostat, e.g., crystals formed only at low temperatures or glassy states formed under extreme conditions and quenched at low temperatures, etc.

Handa has constructed a top-loading Tian–Calvet heat-flow calorimeter in 1984.[1] He measured the heat capacities of various ice and clathrate hydrate systems prepared at low temperature and high pressure,[2–4] but the temperature range was restricted to above 90 K and the accuracy of the C_p measurement was inherently limited by the principle of conduction calorimetry. No top-loading adiabatic calorimeter has been constructed so far. This is because the following complicated structure of an adiabatic calorimeter have been difficult to realize in the top-loading type cryostat; (i) the sample cell is surrounded by double (inner and outer) adiabatic shields, (ii) the temperature differences between the cell and the shields are detected by thermocouples, (iii) there are many thin electrical wires connected to the cell, (iv) most parts of the cell, especially resistance thermometer, are very fragile. Therefore, such unstable samples as described above have been studied only with special type adiabatic calorimeters based on *in situ* sample preparation.[5–7]

We have succeeded in developing a top-loading adiabatic calorimeter for the first time. The structure of the calorimeter and the result of the test experiment on the empty sample cell are described in Secs. II and III, respectively. The heat capacity of (1,3-propanediol)$_{0.5}$(1,2-propanediamine)0.5 was measured in the temperature range 20–290 K and the enthalpy relaxation in its glassy state was also measured near $T_g(=178\ \mathrm{K})$. These measurements were carried out on glassy samples prepared by fast cooling to 77 K outside the cryostat as well as on the samples stabilized in the cryostat. These are described in Sec. IV.

[a]Present address: Institute for Chemical Research, Kyoto University, Uji, Kyoto 611, Japan.
[b]Author to whom correspondence should be addressed; electronic mail: yamamuro@chem.sci.osaka-u.ac.jp
[c]Present address: Department of Chemistry, Graduate School of Science, Kyoto University, Kyoto 606-01, Japan.

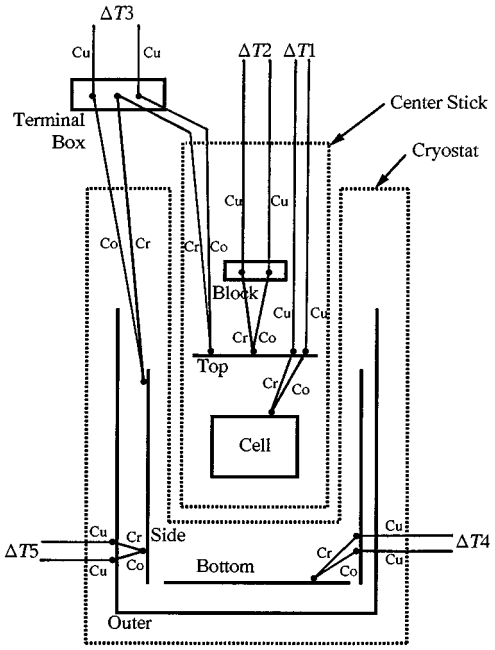

FIG. 1. Block diagram of the adiabatic control system. Two regions surrounded by dotted lines represent the center stick and the main body of the cryostat. Cr, Co, and Cu denote chromel, constantan, and copper wires of the thermocouples, respectively.

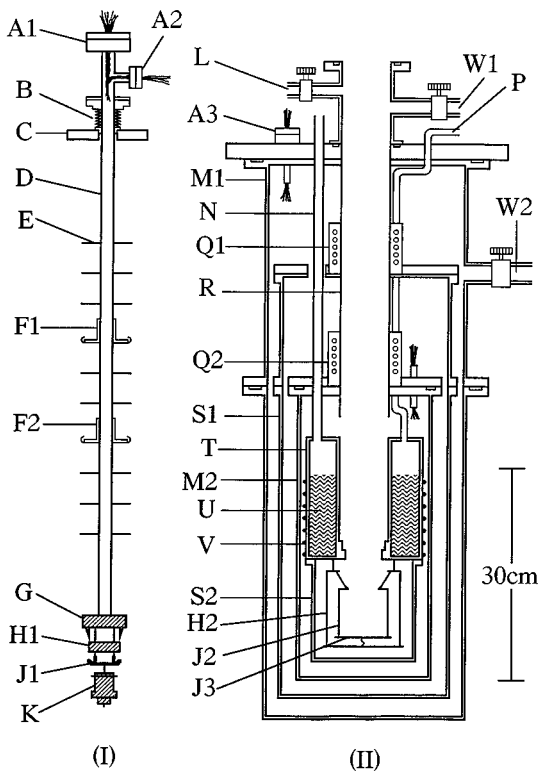

FIG. 2. Schematic drawing of the cryostat: (I) center stick, (II) main body of the cryostat. (A) Hermetic seal connectors, (B) bellows, (C) flange, (D) center stick rod, (E) radiation shielding disks, (F) thermal anchors, (G) thermal anchoring block, (H) outer adiabatic shields (H1: block, H2: outer), (J) inner adiabatic shields (J1: top, J2: side, J3: bottom), (K) sample cell, (L) He gas inlet, (M) vacuum cans, (N) refrigerant filling tube, (P) refrigerant gas outlet, (Q) spiral tubes for cold refrigerant gas, (R) center-stick loading pipe, (S) radiation shields, (T) refrigerant tank, (U) refrigerant, (V) heater wire for refrigerant tank, (W) exhaust tubes.

II. STRUCTURE OF APPARATUS

A. Principle of the adiabatic control

The calorimetric measurement by the top-loading apparatus is based on the usual adiabatic principle.[8] The heat capacity C_p is measured by determining the temperature increment ΔT of the sample caused by electrically supplied energy ΔE under an adiabatic condition; $C_p=\Delta E/\Delta T$. Enthalpy relaxation $\Delta H(T,t)$ is measured by monitoring the spontaneous temperature change dT/dt of the sample as a function of time t under an adiabatic condition; $\Delta H(T,t)=\int C_p(dT/dt)dt$. The adiabatic condition is achieved by evacuating the space surrounding the sample cell and controlling the temperature of the adiabatic shield to the same temperature as the cell.

In the traditional calorimeter, the temperature of the side section of the inner adiabatic shield is controlled against the sample cell and the temperatures of the other sections of the shields against the side section. The temperature control is done by a negative feedback mechanism using a thermocouple, a stable dc amplifier and a power amplifier. Therefore, the sample cell and shield are inevitably connected with each other and with the cryostat by thermocouples and other electrical wires. In a top-loading calorimeter, it is crucial to devise electric circuits that can be connected and disconnected outside the cryostat for setting up of the experiment. The present calorimeter therefore uses a new method for the connection of the thermocouples for the adiabatic control. Figure 1 shows the block diagram of the adiabatic control. Cr, Co, Cu denote chromel, constantan, and copper wires, respectively. The center stick and the cryostat are each surrounded by dotted lines. The sample cell, the top adiabatic shield, and the block (thermal anchor) are included in the center stick part, while the side, bottom, and outer adiabatic shields are in the cryostat part. The top adiabatic shield is controlled against the cell ($\Delta T1$) and the block against the top adiabatic shield ($\Delta T2$). All of the lead wires for the cell heater and thermometer are introduced via the top shield. The bottom and outer adiabatic shields are controlled against the side shield as usual ($\Delta T4$ and $\Delta T5$, respectively). The crucial point of this system is that the temperature control of the side shield is performed using a long thermocouple disconnectable at the terminal box outside the cryostat as shown in the figure ($\Delta T3$).

B. Cryostat

Figure 2 shows schematic drawings of the center stick (I) and the cryostat main body (II). Figure 3 is an expanded view of the sample cell as positioned in the cryostat. The pole of the center stick D is made of stainless steel tube (15 mmϕ), which has good mechanical strength and low thermal conductivity. All of the lead wires pass through this tube and are taken out of the cryostat at the hermetic seals A1 and A2. The cryostat is vacuum sealed by the flange C with a rubber O ring. The bellows B gives the flexibility necessary to push down the center stick for good mechanical and thermal contact between the thermal anchoring copper block G and the

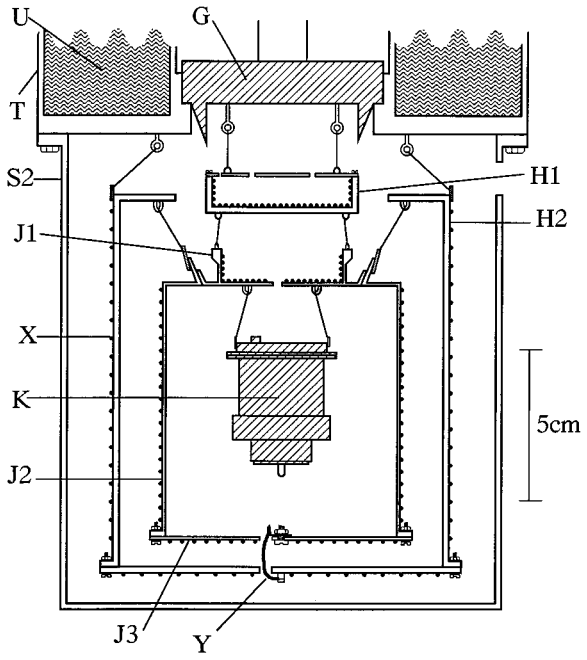

FIG. 3. Expanded view around the sample cell: (G) thermal anchoring block, (H) outer adiabatic shields (H1: block, H2: outer), (J) inner adiabatic shields (J1: top, J2: side, J3: bottom), (K) sample cell, (S) radiation shields, (T) refrigerant tank, (U) refrigerant, (X) heater wire for adiabatic shields, (Y) copper wire.

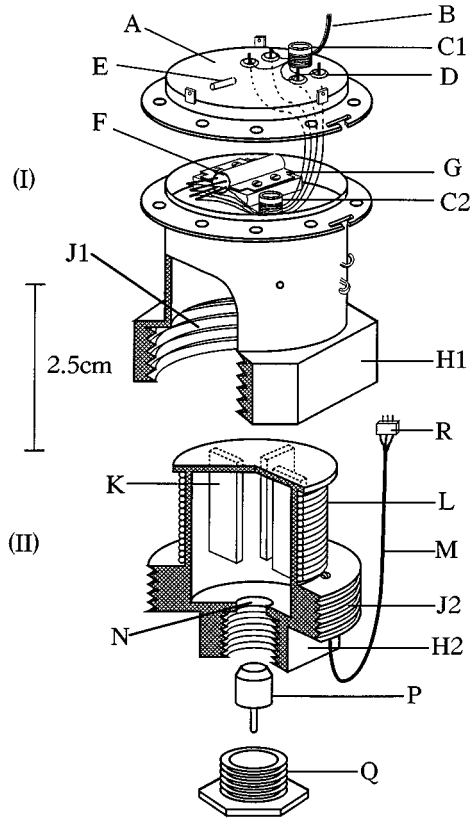

FIG. 4. Sketch of the sample cell: (A) lid of thermometer room, (B) lead wires of thermometer, (C) thermal anchors, (D) hermetically sealed feedthrough, (E) thermocouple sleeve, (F) Rh–Fe resistance thermometer, (G) thermometer holder, (H) clamp edges, (J) screws, (K) vanes, (L) manganin heater wire, (M) lead wires of heater, (N) sample inlet hole, (P) plug, (Q) gland nut, (R) pin connector.

lower central edge of the refrigerant tank T. The disks E are radiation shields and F1 and F2 are thermal anchors for the lead wires. The block G suspends another block H1 (for thermal anchoring), the top adiabatic shields J1 and the sample cell K.

The inner space of the outer vacuum can M1 is partitioned into two spaces by the inner vacuum can M2. The two subspaces can be evacuated separately through W1 and W2 down to 10^{-4} Pa by an oil diffusion pump and an oil rotary pump. S1 and S2 are radiation shields made of aluminum with good thermal conductivity. The outer adiabatic shield H2 are suspended from T and the inner adiabatic shield J2 from H2 with copper wires. All of the adiabatic shields (J1–J3, H1, H2) are made of copper. They are gold plated for reduction of radiative heat transfer and for protection against tarnishing. The chromel–constantan thermocouple junctions for the adiabatic control are fixed to each shield and block as described in the last section. The heater wires X are wound pairwise to reduce inductive interference. The copper wire Y works as a thermal link to release a small amount of heat from the inner shields to the outer shield. This is necessary for stable adiabatic control.

Low temperature is obtained by charging refrigerant U (liquid nitrogen or liquid helium) into the tank T through the filling tube N. Vaporized refrigerant flows through the spiral tube Q wound on the center-stick loading pipe R and escapes through the exit P. This heat exchange mechanism reduces the refrigerant consumption. The manganin heater wire V is energized when one wants to remove the refrigerant quickly.

The center stick is loaded into the inner space of M2 and the pipe R while flow of helium gas from L prevents ambient air from entering into the central channel. When the center stick is positioned correctly, the cryostat is vacuum sealed by the flange C. The sample cell is cooled with heat-exchange helium gas down to a desired temperature and the heat capacity measurement started.

C. Sample cell

Figure 4 shows a sketch of the sample cell, some parts of which are cut open for the sake of visibility. The sample cell consists of two main parts; (I) cell cover and (II) main body. They are made of copper. The inner volume and mass are 9.16 cm^3 and 99.6010 g (cell cover: 43.2673 g, main body: 56.3337 g), respectively. The surface of the cell is gold plated for reduction of radiative heat transfer and for protection against tarnishing.

The Rh–Fe resistance thermometer F (27 Ω at 273 K; Oxford Instruments Ltd.) is fixed to the thermometer holder G. The resistance is measured by the use of an automatic resistance bridge (ASL F700). The thermometer was calibrated on the temperature scale ITS-90.[9] The calibration was extended to 300–380 K against a standard platinum thermometer (25 Ω at 273 K; Chino Corp.). The calibration data were polynomialized by the Chebyshev equation. Deviations from the best fit Chebyshev polynomial were within ± 1.5 mK ($T<27$ K), ± 2.5 mK (27 K$<T<$300 K), and ± 1.5 mK ($T>300$ K). The lead wires B of the thermometer

are wound on the thermal anchor C2, soldered on a hermetically sealed feedthrough D and then wound on another thermal anchor C1. The ends of the wires B are connected to the terminals on the top adiabatic shield. The thermometer is enclosed with heat-exchange helium gas (10^5 Pa at 293 K) by the lid A using an indium O ring and 12 screws. The copper sleeve E accepts the thermocouple junction for the adiabatic control.

A manganin heater wire L (122 Ω) is wound on the outer surface of the body. The ends of the heater wire are connected to the pins of a connector R through copper wire M. The electric current is supplied by a constant-current source. The supplied energy is measured with a digital voltmeter and a clock in the computer. The six vanes K are fixed to the inner wall of the cell body to shorten the thermal path between the heater and the sample.

D. Sample setting

The calorimeter is set up for an ordinary experiment in the following way. The sample is loaded through the hole N, which is vacuum sealed mechanically with the plug P and the gland nut Q. The main body is then connected to the cell cover by a pair of the screws J1 and J2 clamping the edges H1 and H2. The plug P and the part around the hole of the main body (N and H2) are made of copper–beryllium alloy which has high thermal conductivity and mechanical strength. The pin connector R is finally inserted in its counterpart fixed at the top adiabatic shield.

When loading a sample at low temperatures, we use a large glove box (70 cm W×70 cm D×200 cm H) installed at the top of the cryostat. This box, filled with helium gas, covers the space around the center-stick inlet. The center stick is suspended inside the box from the ceiling. The sample, which has been stored at low temperatures, is loaded into the sample cell immersed in liquid nitrogen. The cell is sealed in liquid nitrogen and then screwed quickly into the cell cover also cooled with liquid nitrogen. The cell is immersed into liquid nitrogen again and the pin connector for the heater is set up as described above. Finally, the center stick is inserted into the cryostat which is cooled in advance to liquid nitrogen temperature. The experiment can thus be set up at low temperature since all the procedure is free from indium sealing and soldering, which are time consuming and very difficult to do at liquid nitrogen temperature.

III. HEAT CAPACITY OF EMPTY CELL

As a test experiment, the heat capacity of the cell containing helium gas (0.1 MPa at 290 K) was measured between 13 and 375 K. The temperature increment of the heat capacity measurement was about 1 K at 13 K and increased progressively up to about 3 K at higher temperatures.

Figure 5 shows the heat capacity of the empty cell. These data were fitted with 7–12th-order polynomial functions in three ranges of temperature. Figure 6 gives the percent deviation plot from the fitted curve. The deviations are within ±0.2% between 13 and 30 K, ±0.1% between 30 and 50 K, and ±0.02% above 50 K. This result indicates that the precision of the *net* heat capacity of a sample determined by this apparatus is better than 1% between 13 and 50 K and better than 0.1% above 50 K assuming that the heat capacity of the sample is 20% of the gross heat capacity. The precision is the same as that of the best adiabatic calorimeter. Thus we have developed a top-loading adiabatic calorimeter which has an equivalent performance to that of the traditional adiabatic calorimeter.

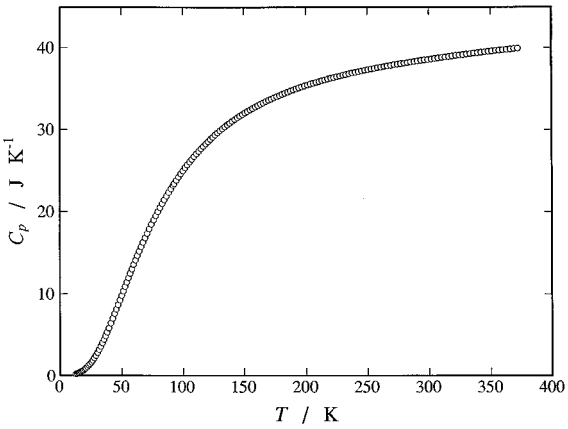

FIG. 5. Heat capacities of the empty cell.

IV. HEAT CAPACITY AND ENTHALPY RELAXATION OF (1,3-PROPANEDIOL)$_{0.5}$(1,2-PROPANEDIAMINE)$_{0.5}$

The structural relaxation in supercooled liquids and glasses is one of the current topics in condensed matter physics and chemistry. One of the powerful methods to investigate this phenomenon is to measure irreversible enthalpy relaxations around a glass transition temperature, where the relaxation time is in the order of 10^2-10^4 s. Such enthalpy relaxations can be observed as a spontaneous temperature increase by use of an adiabatic calorimeter.[10–15] It has been pointed out that the measurement should be done not only as a function of temperature but also as a function of the rate at which the glassy sample was cooled. A glass prepared with a higher cooling rate will have a higher fictive temperature[16] and so have higher enthalpy and entropy, less density, and more disordered local structure. However, the experiments

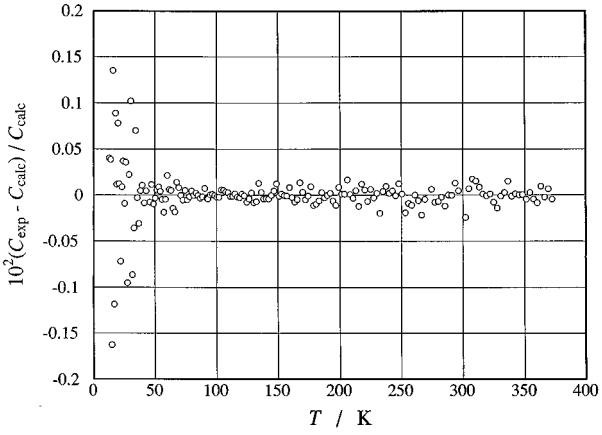

FIG. 6. Deviation plot from the smoothed heat capacity curve of the empty cell.

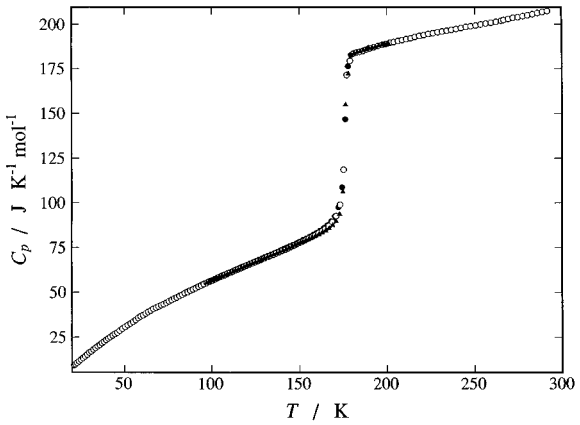

FIG. 7. Heat capacities of the glassy and supercooled states of (1,3-propanediol)$_{0.5}$(1,2-propanediamine)$_{0.5}$ prepared by three different cooling rates. RQG (3 K s^{-1}): closed circles, NQG (1×10^{-2} K s^{-1}): open circles, SQG (8×10^{-4} K s^{-1}): closed triangles.

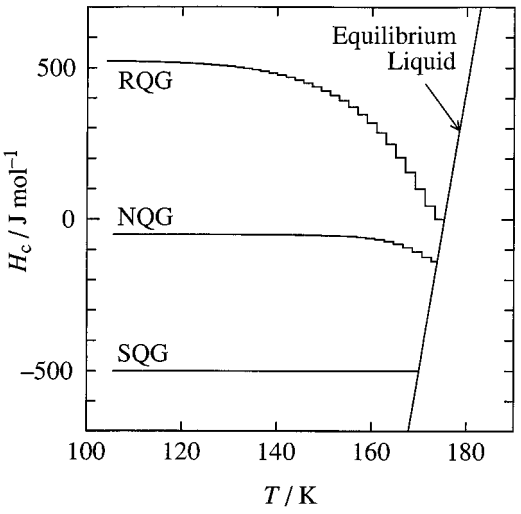

FIG. 8. Configurational enthalpy relaxation paths during the heat capacity measurements of (1,3-propanediol)$_{0.5}$(1,2-propanediamine)$_{0.5}$ prepared by three different cooling rates. See text for the details of the graph.

over a wide range of cooling rate have not been possible since the maximum rate available in traditional adiabatic calorimeters is at most about 0.1 K s^{-1}.

By use of the present calorimeter, we have succeeded in measuring the heat capacities and enthalpy relaxations of glassy samples prepared with cooling rates varied over four decades. The sample material was a recently found glass-forming molecular liquid (1,3-propanediol)$_{0.5}$ (1,2-propanediamine)$_{0.5}$, which does not crystallize all over the temperature region between $T_g(=178\ \mathrm{K})$ and fusion temperature.[17] This sample is abbreviated as PDO-PDA hereafter.

The details of the sample purification and mixing procedure are described elsewhere.[17] The precise mole fraction of the sample was (1,3-propanediol)$_{0.49903}$(1,2-propanediamine)$_{0.50097}$ and the mass of the sample loaded in the sample cell was 8.512 62 g (0.113 34 mol). We have prepared three samples with different cooling rates: rapidly quenched glass (RQG) (cooling rate: 3 K s^{-1} around T_g), normally quenched glass (NQG) (1×10^{-2} K s^{-1}), and slowly quenched glass (SQG) (8×10^{-4} K s^{-1}). The RQG sample was prepared by immersing the filled sample cell into liquid nitrogen and then loaded into the cryostat. This method is of course impossible in traditional adiabatic calorimeters. Both NQG and SQG samples were prepared by cooling the filled sample cell inside the cryostat as usual.

Figure 7 shows the heat capacities of the PDO-PDA samples prepared with three different cooling rates. The heat capacity curves of the three samples were almost the same including the portion at the glass transition temperature. Heat capacity of a glass is directly related to its vibrational density of states except near the glass transition. Therefore, this result indicates that the vibrational states at higher frequencies, contributing to the present heat capacity, are not affected much by the local structure and density.

Figure 8 shows the plot of the configurational enthalpy versus temperature. The steplike lines represent the enthalpy paths taken by the sample during the heat capacity measurements. The horizontal segments represent the temperature increases caused by supplying energy and the vertical ones the exothermic enthalpy relaxations. The method to calculate the relaxed enthalpy is described elsewhere.[18] The curve smoothly rising up to the right gives the hypothetical equilibrium configurational enthalpy derived by integrating the heat capacity difference between the glassy and liquid states. The point of intersection of the steplike line and equilibrium curve corresponds to the glass transition temperature of each sample. The zero of ΔH_c was taken at the glass transition temperature of RQG sample. As we expected, the total enthalpy relaxed in RQG was much larger than that of NQG. Interestingly and unexpectedly RQG started to relax far below T_g while SQG did not relaxed up to T_g. In adiabatic calorimetry, the enthalpy relaxation starts at the temperature where the α relaxation time τ_α reaches about 10^4 s. Hence the present results have shown that $\tau_\alpha(\mathrm{RQG})\ll\tau_\alpha(\mathrm{NQG})\ll\tau_\alpha(\mathrm{SQG})$, indicating that the α relaxation is drastically accelerated by the disordered and/or less dense local structure. We are now analyzing this data and the similar data recently obtained on glycerol[19] by using the Adam–Gibbs theory[20] which involves the effect of short-range ordering on the α relaxation.

ACKNOWLEDGMENTS

This work is financially supported by the Ministry of Education, Science and Culture, Japan Grant-in-Aid for Scientific Research on Priority Areas No. 07236230 and Grant-in-Aid for Scientific Research No. 06804032. We thank Masahiro Shiomi and Shoji Ishimoto of the Metal Work Division of the Central Workshop of Osaka University for their great help in constructing the apparatus.

[1] Y. P. Handa, R. E. Hawkins, and J. J. Murray, J. Chem. Thermodyn. **16**, 623 (1984).
[2] Y. P. Handa, O. Mishima, and E. Whalley, J. Chem. Phys. **84**, 2766 (1986).
[3] Y. P. Handa, J. Chem. Thermodyn. **18**, 891 (1986).
[4] Y. P. Handa, J. Chem. Thermodyn. **18**, 915 (1986).
[5] M. Oguni, K. Watanabe, T. Matsuo, H. Suga, and S. Seki, Bull. Chem. Soc. Jpn. **55**, 77 (1982).

[6] O. Yamamuro, M. Oguni, T. Matsuo, and H. Suga, Bull. Chem. Soc. Jpn. **60**, 1269 (1987).
[7] H. Hikawa, M. Oguni, and H. Suga, J. Non-Cryst. Solids **101**, 90 (1988).
[8] E. F. Westrum, Jr., G. T. Furukawa, and J. P. McCullough, *Experimental Thermodynamics*, edited by J. P. McCullough and D. W. Scott (Butterworths, London, 1968), Vol. 1, Chap. 5.
[9] R. N. Goldberg and R. D. Weir, Pure Appl. Chem. **64**, 1545 (1992).
[10] K. Takeda, O. Yamamuro, and H. Suga, J. Phys. Chem. Solids **52**, 607 (1991).
[11] K. Takeda, O. Yamamuro, and H. Suga, J. Phys. Chem. **99**, 1602 (1995).
[12] I. Tsukushi, O. Yamamuro, and H. Suga, J. Non-Cryst. Solids **175**, 187 (1994).
[13] O. Yamamuro, S. Takahara, and H. Suga, J. Non-Cryst. Solids **183**, 144 (1995).
[14] I. Tsukushi, O. Yamamuro, T. Ohta, T. Matsuo, H. Nakano, and Y. Shirota, J. Phys. Condens. Matter **8**, 245 (1996).
[15] H. Fujimori, Y. Adachi, and M. Oguni, Phys. Rev. B **46**, 14 501 (1992).
[16] A. Q. Tool and C. G. Eichlin, J. Am. Chem. Soc. **54**, 491 (1931).
[17] K. Takeda, K. Murata, and S. Yamashita (unpublished).
[18] For example, K. Okishiro, O. Yamamuro, T. Matsuo, S. Nishikiori, and T. Iwamoto, J. Phys. Chem. B **101**, 5804 (1997).
[19] O. Yamamuro and T. Matsuo, J. Non-Cryst. Solids (in press).
[20] G. Adam and J. H. Gibbs, J. Chem. Phys. **43**, 139 (1965).